

# Low Probability of Intercept Frequency Hopping Signal Characterization Comparison using the Spectrogram and the Scalogram 1

Daniel L. Stevens<sup>1</sup> and Stephanie A. Schuckers<sup>2</sup>

<sup>1</sup> Clarkson University

*Received: 9 December 2015 Accepted: 1 January 2016 Published: 15 January 2016*

---

## Abstract

Low probability of intercept radar signals, which are often problematic to detect and characterize, have as their goal ?to see and not be seen?. Digital intercept receivers are currently moving away from Fourier-based analysis and towards classical time-frequency analysis techniques for the purpose of analyzing these low probability of intercept radar signals. This paper presents the novel approach of characterizing low probability of intercept frequency hopping radar signals through utilization and direct comparison of the Spectrogram versus the Scalogram. Two different frequency hopping low probability of intercept radar signals were analyzed(4-component and 8-component). The following metrics were used for evaluation: percent error of: carrier frequency, modulation bandwidth, modulation period, and timefrequency localization. Also used were: percent detection, lowest signal-to-noise ratio for signal detection, and plot (processing) time. Experimental results demonstrate that overall, the Scalogram produced more accurate characterization metrics than the Spectrogram. An improvement in performance may well translate into saved equipment and lives.

---

*Index terms—*

## 1 I. Introduction

low probability of intercept (LPI) radar that uses frequency hopping techniques changes the transmitting frequency in time over a wide bandwidth in order to prevent an intercept receiver from intercepting the waveform. The frequency slots used are chosen from a frequency hopping sequence, and it is this unknown sequence that gives the radar the advantage over the intercept receiver in terms of processing gain. The frequency sequence appears random to the intercept receiver, and so the possibility of it following the changes in frequency is remote [PAC09]. This prevents a jammer from reactively jamming the transmitted frequency [ADA04]. Frequency hopping radar performance depends only slightly on the code used, given that certain properties are met. This allows for a larger variety of codes, making it more difficult to intercept.

Time-frequency signal analysis involves the analysis and processing of signal  $s$  with time -varying The STFT of a signal  $??(??)$  is given in equation 1 as:  $??(??, \delta ??" \delta ??"; ?) = ? ??(??)? +? ??(?? ? ??)?? ???$   $???\delta ??" \delta ??"?? ??? (1)$

Where  $?(??)$  is a short time analysis window localized around  $?? = 0$  and  $\delta ??" \delta ??" = 0$ . Because multiplication by the relatively short window  $?(?? ? ??)$  effectively suppresses the signal outside a neighborhood around the analysis point  $?? = ??$ , the STFT is a 'local' spectrum of the signal  $??(??)$  around  $??$ . Think of the window  $?(??)$  as sliding along the signal  $??(??)$  and for each shift  $?(?? ? ??)$  we compute the usual Fourier transform of the product function  $??(??)?(?? ? ??)$ . The observation window allows localization of the spectrum in time, but also smears the spectrum in frequency in accordance with the uncertainty principle, leading to a trade-off between time resolution and frequency resolution. In general, if the window is short, the time resolution is good,

43 but the frequency resolution is poor, and if the window is long, the frequency resolution is good, but the time  
44 resolution is poor.

45 The STFT was the first tool devised for analyzing a signal in both time and frequency simultaneously. For  
46 analysis of human speech, the main method was, and still is, the STFT. In general, the STFT is still the most  
47 widely used method for studying non-stationary signals [COH95].

48 The Spectrogram (the squared modulus of the STFT) is given by equation 2 as:  $S(f, t) = |STFT(x(t), h(t - \tau))|^2$   
49  $(f, t) = \int_{-\infty}^{\infty} |STFT(x(t), h(t - \tau))|^2 d\tau$  (2)

50 The Spectrogram is a real-valued and nonnegative distribution. Since the window  $h$  of the STFT is assumed  
51 of unit energy, the Spectrogram satisfies the global energy distribution property. Thus we can interpret the  
52 Spectrogram as a measure of the energy of the signal contained in the time-frequency domain centered on the  
53 point  $(t, f)$  and whose shape is independent of this localization.

54 Here are some properties of the Spectrogram: 1) Time and Frequency covariance -The Spectrogram preserves  
55 time and frequency shifts, thus the spectrogram is an element of the class of quadratic time-frequency distributions  
56 that are covariant by translation in time and in frequency (i.e. Cohen's class); 2) Time-Frequency Resolution -The  
57 time-frequency resolution of the Spectrogram is limited exactly as it is for the STFT; there is a trade-off between  
58 time resolution and frequency resolution. This poor resolution is the main drawback of this representation; 3)  
59 Interference Structure -As it is a quadratic (or bilinear) representation, the Spectrogram of the sum of two signals  
60 is not the sum of the two Spectrograms (quadratic superposition principle); there is a cross-Spectrogram part  
61 and a real part. Thus, as for every quadratic distribution, the Spectrogram presents interference terms; however,  
62 those interference terms are restricted to those regions of the time-frequency plane where the signals overlap.  
63 Thus if the signal components are sufficiently distant so that their Spectrograms do not overlap significantly,  
64 then the interference term will nearly be identically zero [ISI96], [COH95], [HLA92].

65 The Scalogram is defined as the magnitude squared of the wavelet transform, and can be used as a time-  
66 frequency distribution [COH02], [GAL05], [BOA03].

67 The idea of the wavelet transform (equation (3)) is to project a signal  $x(t)$  on a family of zero-mean functions  
68 (the wavelets) deduced from an elementary function (the mother wavelet) by translations and dilations:  $\psi(t) = \int_{-\infty}^{\infty} \psi(t - \tau) \delta(t - \tau) d\tau$   
69  $(\psi, \psi; ?) = \int_{-\infty}^{\infty} \psi(t) \psi(t - \tau) \delta(t - \tau) d\tau$  (3)

70 Where  $\int_{-\infty}^{\infty} \psi(t) \psi(t - \tau) \delta(t - \tau) d\tau = |\psi(t)|^2$

## 71 2 ??

72 . The wavelet transform is of interest for the analysis of non-stationary signals, because it provides still another  
73 alternative to the STFT and to many of the quadratic time-frequency distributions. The basic difference between  
74 the STFT and the wavelet transform is that the STFT uses a fixed signal analysis window, whereas the wavelet  
75 transform uses short windows at high frequencies and long windows at low frequencies. This helps to diffuse  
76 the effect of the uncertainty principle by providing good time resolution at high frequencies and good frequency  
77 resolution at low frequencies. This approach makes sense especially when the signal at hand has high frequency  
78 components for short durations and low frequency components for long durations. The signals encountered in  
79 practical applications are often of this type.

80 The wavelet transform allows localization in both the time domain via translation of the mother wavelet, and  
81 in the scale (frequency) domain via dilations. The wavelet is irregular in shape and compactly supported, thus  
82 making it an ideal tool for analyzing signals of a transient nature; the irregularity of the wavelet basis lends itself  
83 to analysis of signals with discontinuities or sharp changes, while the compactly supported nature of wavelets  
84 enables temporal localization of a signal's features [BOA03]. Unlike many of the quadratic functions such as  
85 the Wigner-Ville Distribution (WVD) and Choi-Williams Distribution (CWD), the wavelet transform is a linear  
86 transformation, therefore cross-term interference is not generated. There is another major difference between the  
87 STFT and the wavelet transform; the STFT uses sines and cosines as an orthogonal basis set to which the signal  
88 of interest is effectively correlated against, whereas the wavelet transform uses special 'wavelets' which usually  
89 comprise an orthogonal basis set. The wavelet transform then computes coefficients, which represents a measure  
90 of the similarities, or correlation, of the signal with respect to the set of wavelets. In other words, the wavelet  
91 transform of a signal corresponds to its decomposition with respect to a family of functions obtained by dilations  
92 (or contractions) and translations (moving window) of an analyzing wavelet.

93 A filter bank concept is often used to describe the wavelet transform. The wavelet transform can be interpreted  
94 as the result of filtering the signal with a set of bandpass filters, each with a different center frequency [GRI08],  
95 [FAR96], [SAR98], [SAT98].

96 Like the design of conventional digital filters, the design of a wavelet filter can be accomplished by using a  
97 number of methods including weighted least squares [ALN00], [GOH00], orthogonal matrix methods [ZAH99],  
98 nonlinear optimization, optimization of a single parameter (e.g. the passband edge) [ZHA00], and a method that  
99 minimizes an objective function that bounds the out-of-tile energy [FAR99].

100 Here are some properties of the wavelet transform: 1) The wavelet transform is covariant by translation in  
101 time and scaling. The corresponding group of transforms is called the Affine group; 2) The signal  $x(t)$  can be  
102 recovered from its wavelet transform via the synthesis wavelet; 3) Time and frequency resolutions, like in the  
103 STFT case, are related via the Heisenberg-Gabor inequality. However in the wavelet transform case, these two  
104 resolutions depend on the frequency: the frequency resolution becomes poorer and the time resolution becomes

---

105 better as the analysis frequency grows;4) Because the wavelet transform is a linear transform, it does not contain  
106 cross-term interferences[GRI07], [LAR92].

107 A similar distribution to the Spectrogram can be defined in the wavelet case. Since the wavelet transform  
108 behaves like an orthonormal basis decomposition, it can be shown that it preserves energy:  $|\int \psi(x) \psi^*(x) dx|$   
109  $2 + \int \psi(x) \psi^*(x) dx = 2$  (4)

110 where  $\int \psi(x) \psi^*(x) dx$  is the energy of  $\psi$ . This leads us to define the Scalogram (equation (4)) of  $\psi$  as the squared  
111 modulus of the wavelet transform. It is an energy distribution of the signal in the time-scale plane, associated  
112 with the measure  $\int \psi(x) \psi^*(x) dx$ . As is the case for the wavelet transform, the time and frequency resolutions of the  
113 Scalogram are related via the Heisenberg-Gabor principle.

114 The interference terms of the Scalogram, as for the spectrogram, are also restricted to those regions of the  
115 time-frequency plane where the corresponding signals overlap. Therefore, if two signal components are sufficiently  
116 far apart in the time-frequency plane, their cross-Scalogram will be essentially zero [ISI96], [HLA92].

117 For this paper, the Morlet Scalogram will be used. The Morlet wavelet is obtained by taking a complex sine  
118 wave and by localizing it with a Gaussian envelope. The Mexican hat wavelet isolates a single bump of the Morlet  
119 wavelet. The Morlet wavelet has good focusing in both time and frequency [CHE09].

## 120 3 II. Methodology

121 The methodologies detailed in this section describe the processes involved in obtaining and comparing metrics  
122 between the classical time-frequency analysis techniques of the Spectrogram and the Scalogram for the detection  
123 and characterization of low probability of intercept frequency hopping radar signals.

124 The tools used for this testing were: MATLAB (version 7.12), Signal Processing Toolbox (version 6.15),  
125 Wavelet Toolbox (version 4.7), Image Processing Toolbox (version 7.2), Time-Frequency Toolbox (version 1.0)  
126 (<http://tftb.nongnu.org/>).

127 All testing was accomplished on a desktop computer (HP Compaq, 2.5GHz processor, AMD Athlon 64X2  
128 Dual Core Processor 4800+, 2.00GB Memory (RAM), 32 Bit Operating System).

129 Testing was performed for 2 different waveforms (4 component frequency hopping, 8 component frequency  
130 hopping). For each waveform, parameters were chosen for academic validation of signal processing techniques.  
131 Due to computer processing resources they were not meant to represent real-world values. The number of samples  
132 for each test was chosen to be 512, which seemed to be the optimum size for the desktop computer. Testing  
133 was performed at three different SNR levels: 10dB, 0dB, and the lowest SNR at which the signal could be  
134 detected. The noise added was white Gaussian noise, which best reflects the thermal noise present in the IF  
135 section of an intercept receiver [PAC09]. Kaiser windowing was used, when windowing was applicable. 50 runs  
136 were performed for each test, for statistical purposes. The plots included in this paper were done at a threshold  
137 of 5% of the maximum intensity and were linear scale (not dB) of analytic (complex) signals; the color bar  
138 represented intensity. The signal processing tools used for each task were the Spectrogram and the Scalogram.

139 Task 1 consisted of analyzing a frequency hopping (prevalent in the LPI arena [AMS09]) 4component signal  
140 whose parameters were: sampling frequency=5KHz; carrier frequencies=1KHz, 1.75KHz, 0.75KHz, 1.25KHz;  
141 modulation bandwidth=1KHz; modulation period=.025sec.

142 Task 2 was similar to Task 1, but for a frequency hopping 8-component signal whose parameters were: sampling  
143 frequency=5KHz; carrier frequencies=1.5 KHz, 1KHz, 1.25KHz, 1.5KHz, 1.75KHz, 1.25KHz, 0.75KHz, 1KHz;  
144 modulation bandwidth=1KHz; modulation period=.0125sec.

145 After each particular run of each test, metrics were extracted from the time-frequency representation. The  
146 different metrics extracted were as follows: 1) Plot (processing) time: Time required for plot to be displayed.  
147 For visually detected low SNR plots (like this one), the percent of max intensity for the peak z-value of each  
148 of the signal components was noted (here 98%, 78%, 75%, 63%), and the lowest of these 4 values was recorded  
149 (63%). Ten test runs were performed for both timefrequency analysis tools (Spectrogram and Scalogram) for  
150 this waveform. The average of these recorded low values was determined and then assigned as the threshold for  
151 that particular time-frequency analysis tool. Note -the threshold for the Spectrogram is 60%.

152 Thresholds were assigned as follows: Spectrogram (60%); Scalogram (50%).

153 For percent detection determination, these threshold values were included in the time-frequency plot algorithms  
154 so that the thresholds could be applied automatically during the plotting process. From the threshold plot, the  
155 signal was declared a detection if any portion of each of the signal components was visible (see Figure 2).

## 156 4 4) Modulation bandwidth:

157 Distance from highest frequency value of signal (at a threshold of 20% maximum intensity) to lowest frequency  
158 value of signal (at same threshold) in Y-direction (frequency).

159 The threshold percentage was determined based on manual measurement of the modulation bandwidth of  
160 the signal in the time-frequency representation. This was accomplished for ten test runs of each time-frequency  
161 analysis tool (Spectrogram and Scalogram), for each of the 2 waveforms. During each manual measurement, the  
162 max intensity of the high and low measuring points was recorded. The average of the max intensity values for  
163 these test runs was 20%. This was adopted as the threshold value, and is representative of what is obtained when

164 performing manual measurements. This 20% threshold was also adapted for determining the modulation period  
 165 and the time-frequency localization (both are described below).

166 For modulation bandwidth determination, the 20% threshold value was included in the time-frequency plot  
 167 algorithms so that the threshold could be applied automatically during the plotting process. From the threshold  
 168 plot, the modulation bandwidth was manually measured (see Figure 4). ) with threshold value automatically  
 169 set to 20%. From this threshold plot, the time-frequency localization was measured manually from the top of  
 170 the signal (top red arrow) to the bottom of the signal (bottom red arrow) in the y-direction (frequency). This  
 171 frequency 'thickness' value was then converted to: % of entire y-axis.

## 172 5 7) Lowest detectable SNR:

173 The lowest SNR level at which at least a portion of each of the signal components exceeded the set threshold  
 174 listed in the percent detection section above.

175 For lowest detectable SNR determination, these threshold values were included in the time-frequency plot  
 176 algorithms so that the thresholds could be applied automatically during the plotting process. From the threshold  
 177 plot, the signal was declared a detection if any portion of each of the signal components was visible. The lowest  
 178 SNR level for which the signal was declared a detection is the lowest detectable SNR (see Figure 7). 2dB with  
 179 threshold value automatically set to 60%. From this threshold plot, the signal was declared a (visual) detection  
 180 because at least a portion of each of the 4 frequency hopping signal components was visible. For this case, any  
 181 lower SNR would have been a non-detect. Compare to Figure 2, which is the same plot, except that it has an  
 182 SNR level equal to 10dB.

183 The data from all 50 runs for each test was used to produce the actual, error, and percent error for each of  
 184 these metrics listed above. large, the Scalogram outperformed the Spectrogram, as will be shown in the results  
 185 section. From Table 1, the Scalogram outperformed the Spectrogram in average percent error: carrier frequency  
 186 (0.44% vs. 0.67%), modulation bandwidth (21.62% vs. 25.70%), modulation period (10.25% vs. 11.37%), and  
 187 time-frequency (y-direction) (9.44% vs. 9.77%); and in average: percent detection (80.84% vs. 69.67%), and  
 188 lowest detectable SNR (-3.0db vs. -2.0db), while the Spectrogram outperformed the Scalogram in average plot  
 189 time (3.43s vs. 5.62s).

## 190 6 III. Results

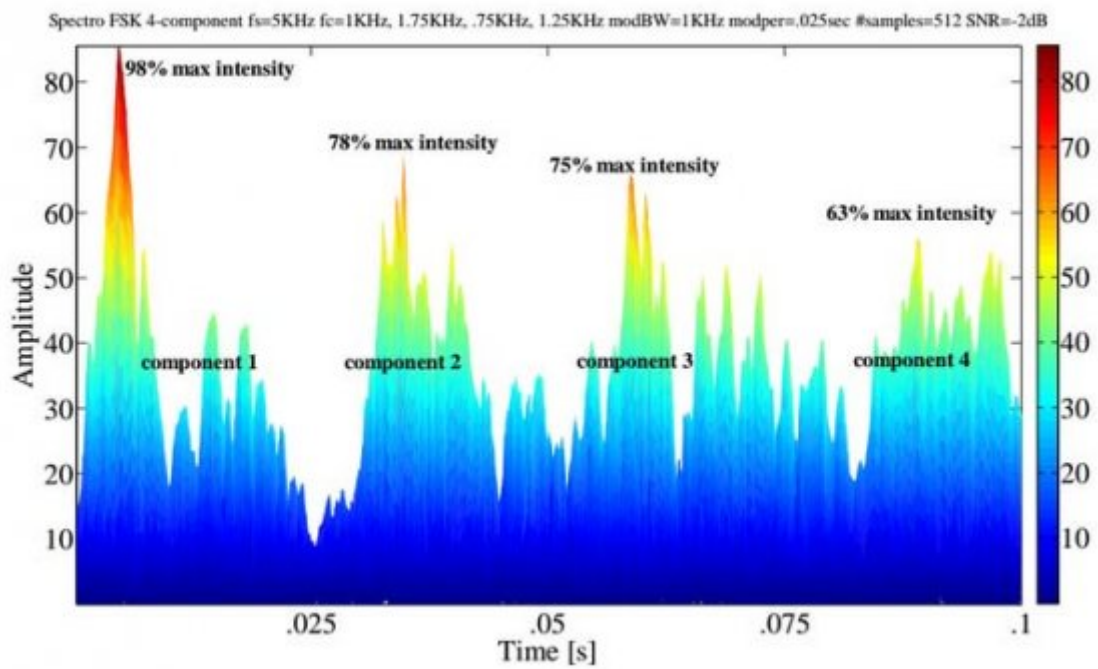
## 191 7 IV. Discussion

192 This section will elaborate on the results from the previous section.

193 From Table 1, the performance of the Spectrogram and the Scalogram will be summarized, including strengths,  
 194 weaknesses, and generic scenarios in which each particular signal analysis tool might be used. Spectrogram: The  
 195 Spectrogram outperformed the Scalogram in average plot time (3.43s vs 5.62s). However, the Spectrogram was  
 196 outperformed by the Scalogram in every other category. The Spectrogram's extreme reduction of cross-term  
 197 interference is grounds for its good plot time, but at the expense of signal localization (i.e. it produces a 'thicker'  
 198 signal (as is seen in Figure 8 and Figure 9) -due to the trade-off between cross-term interference and signal  
 199 localization). This poor signal localization ('thicker' signals) can account for the Spectrogram being outperformed  
 200 in the areas of average percent error of modulation bandwidth, modulation period, and time-frequency localization  
 201 (ydirection). The spectrogram might be used in a scenario where a short plot time is necessary, and where signal  
 202 localization is not an issue. Such a scenario might be a 'quick and dirty' check to see if a signal is present, without  
 203 precise extraction of its parameters. Scalogram: The Scalogram outperformed the Spectrogram in every category  
 204 but plot time. Because of the Spectrogram's extreme reduction of cross-terms at the expense of signal localization  
 205 (i.e. it produces a 'thicker' signal), the Scalogram was more localized than the Spectrogram, accounting for its  
 206 better performance in the areas of average percent error of modulation bandwidth, modulation period, and  
 207 time-frequency localization (y-direction). In addition, since the compactly supported nature of the wavelet (basis  
 208 of Scalogram) enables temporal localization of a signal's features, this may also have contributed to the the  
 209 Scalogram's better average percent error of modulation period. Average percent detection and lowest detectable  
 210 SNR are both based on visual detection in the Time-Frequency representation. Figures 8 and 9 clearly show  
 211 that the signals in the Scalogram plots are more readable than those in the Spectrogram plots, which accounts  
 212 for the Scalogram's better average percent detection and lowest detectable SNR. Since the irregularity of the  
 213 wavelet basis (basis of Scalogram) lends itself to analysis of signals with discontinuities (such as the frequency  
 214 hopping signals used in this testing), this may have been a contributing factor to the Scalogram's better overall  
 215 performance versus the Spectrogram. Also, since the wavelet is irregular in shape and compactly supported, it  
 216 makes it an ideal tool for analyzing signals of transient nature (such as the frequency hopping signals used in this  
 217 testing), which may also have been a contributing factor to the Future plans include analysis of an additional  
 218 low probability of intercept radar waveform (triangular modulated FMCW), again using the Spectrogram and  
 219 the Scalogram as time-frequency analysis techniques.



Figure 1:



2

Figure 2: 2 )

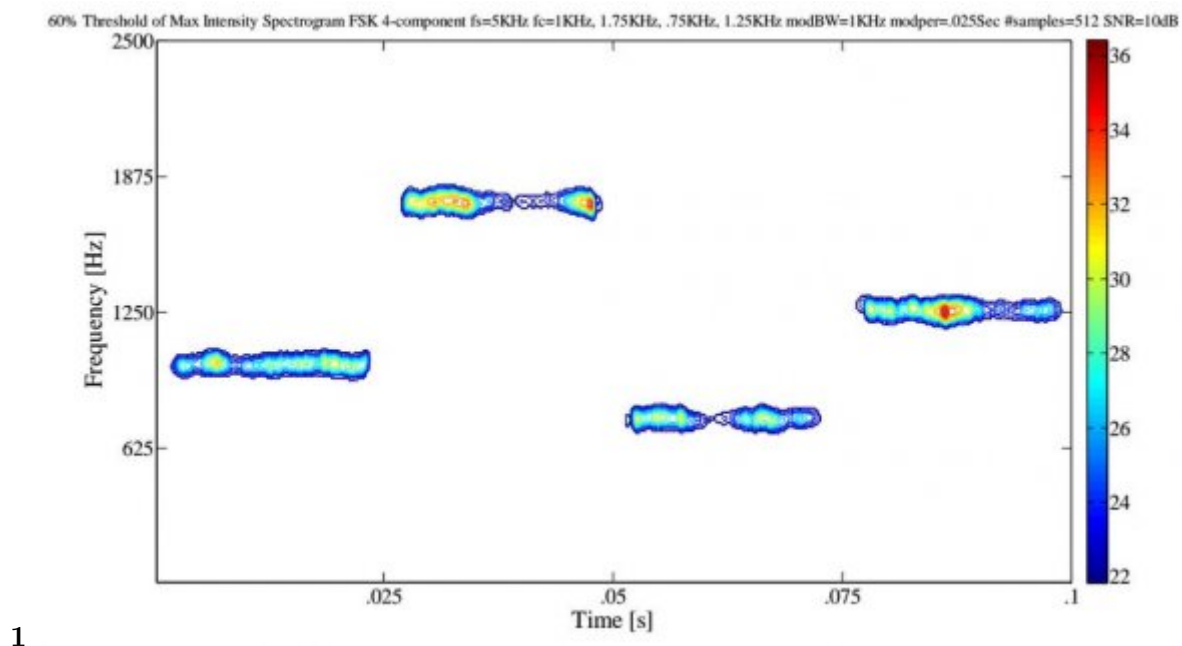


Figure 3: Figure 1 :

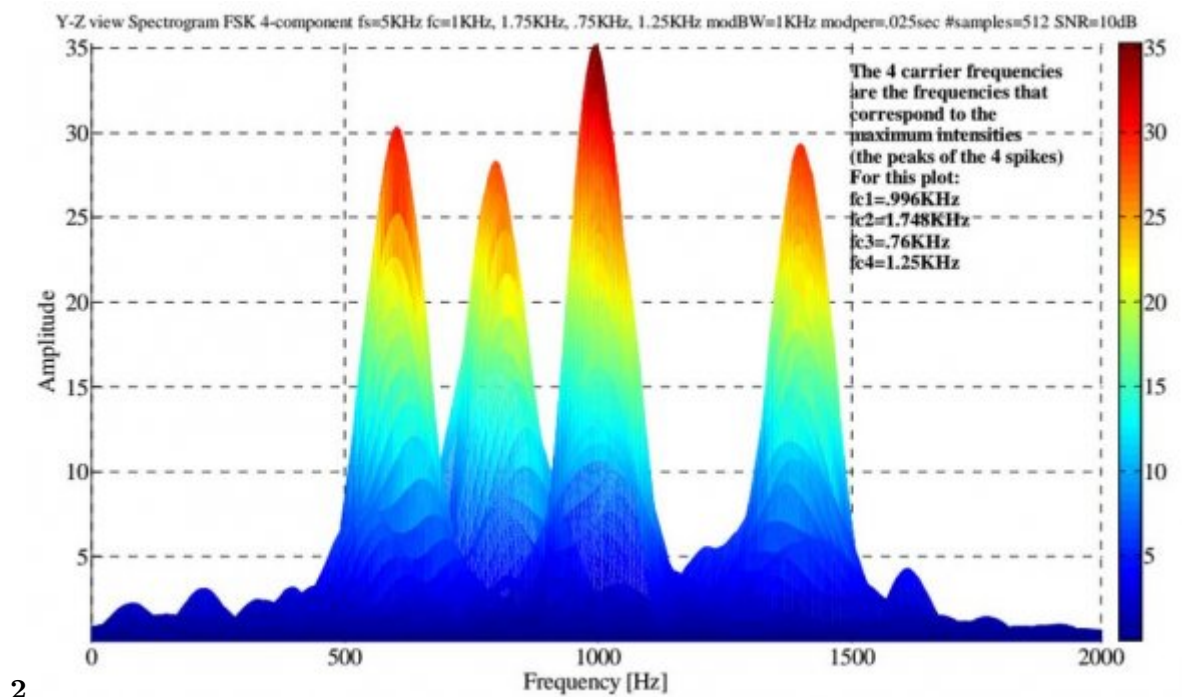


Figure 4: Figure 2 :

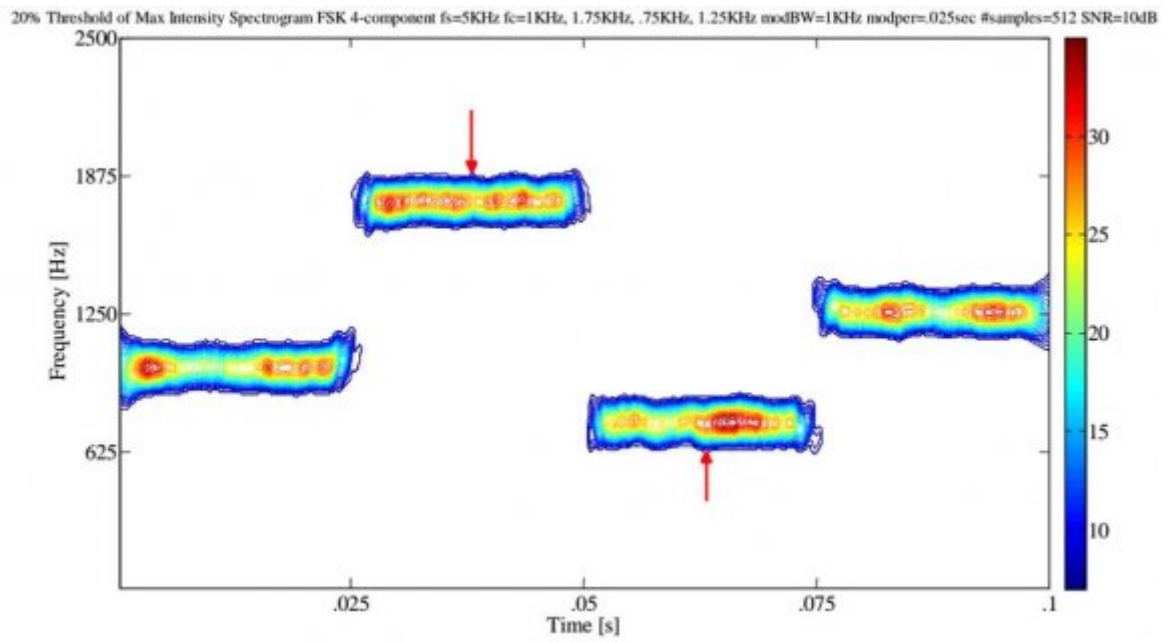


Figure 5: Figure 3 :

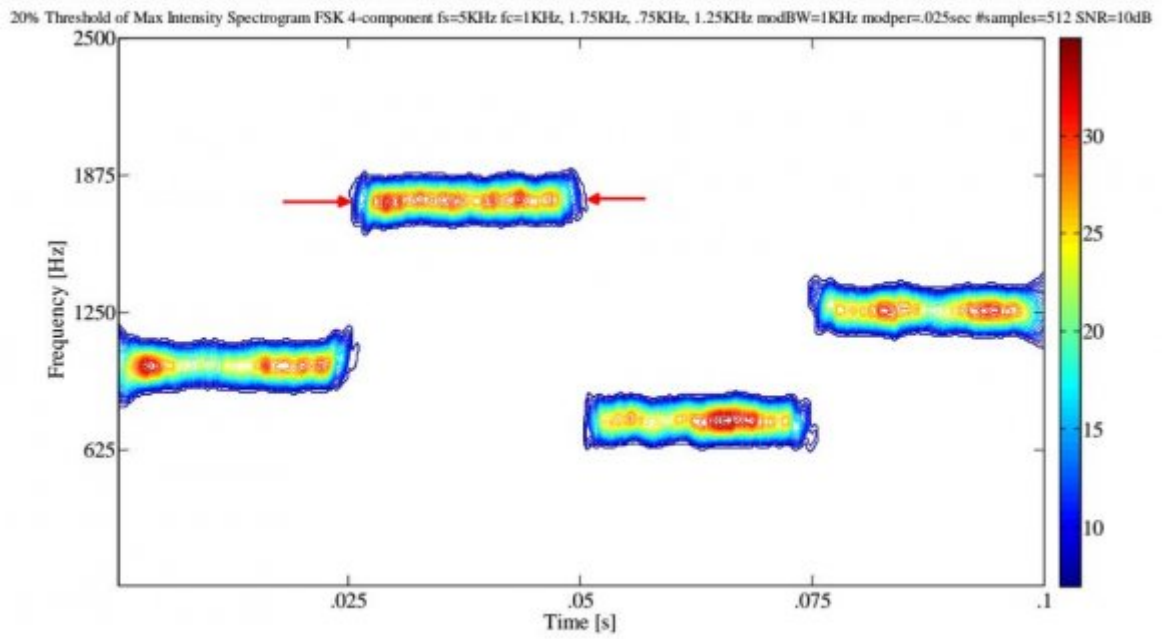


Figure 6: Figure 4 :

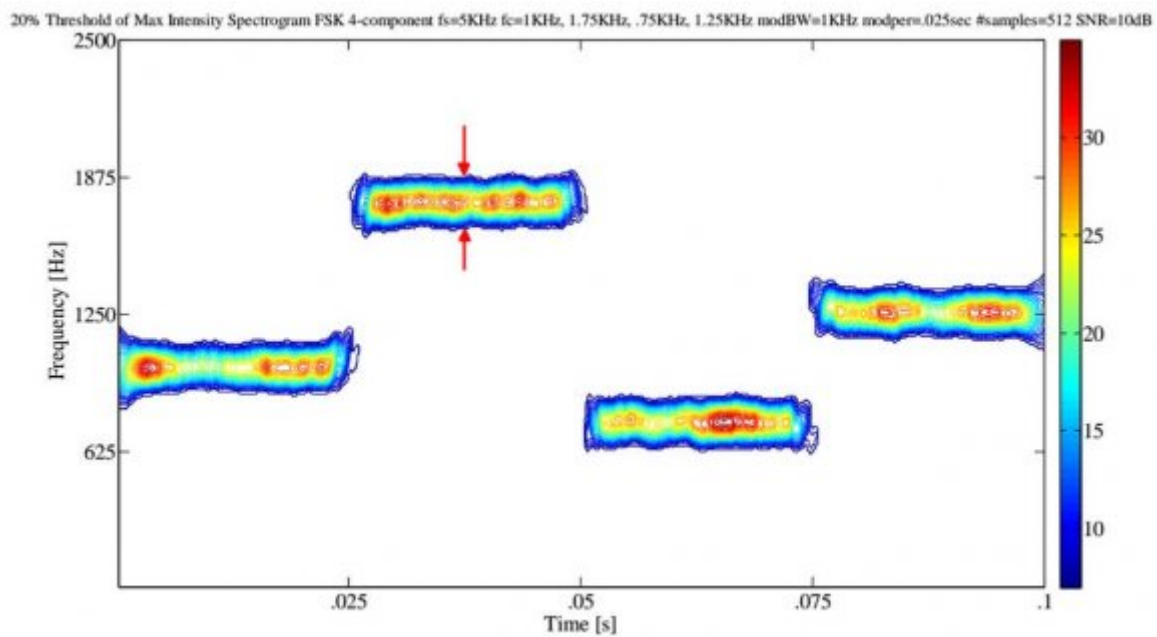


Figure 7: Figure 5 :

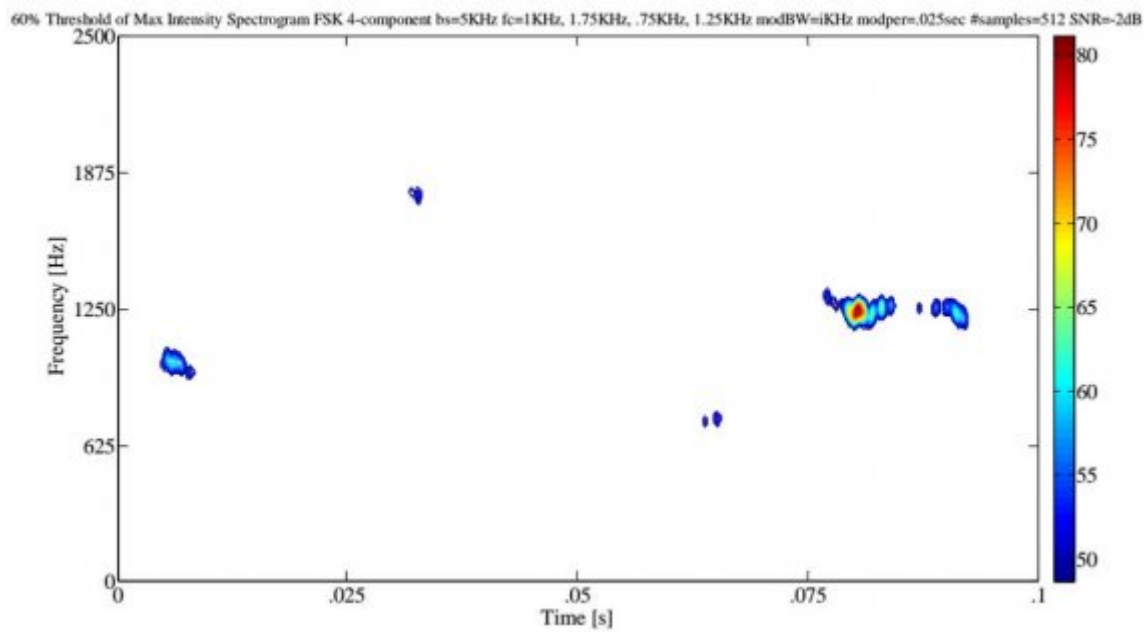
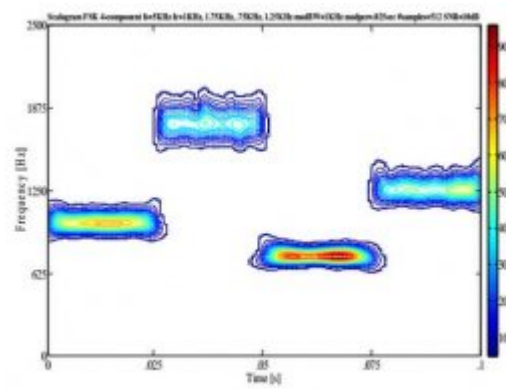
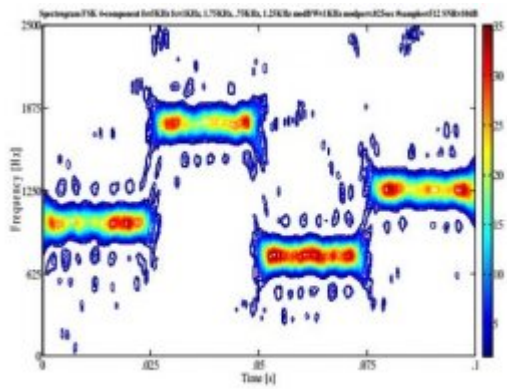
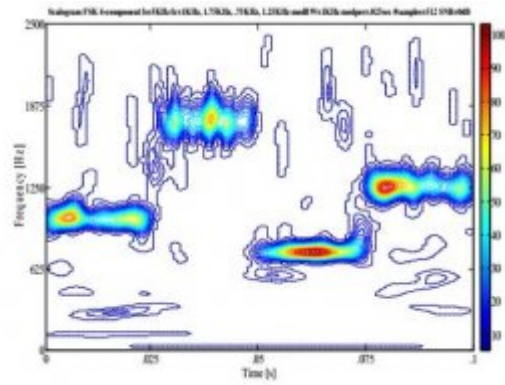
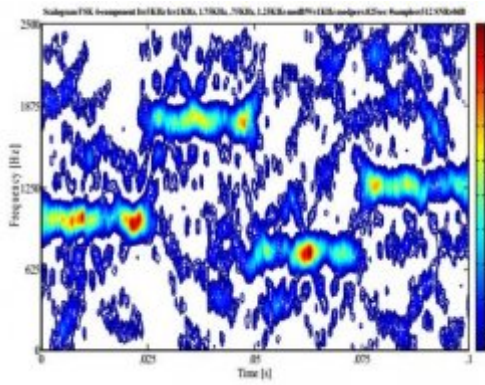


Figure 8: Figure 6 :



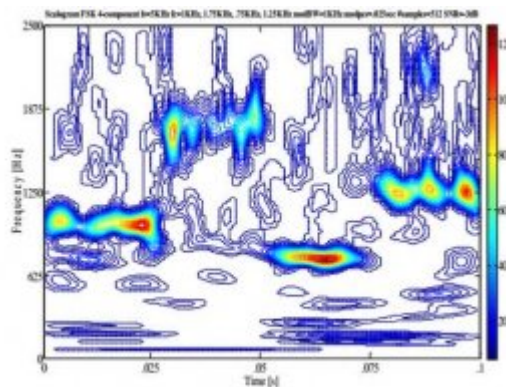
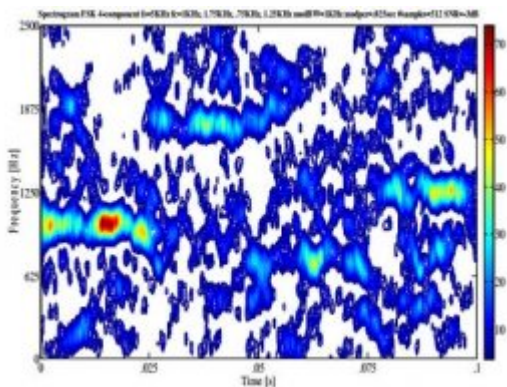
7

Figure 9: Figure 7 :



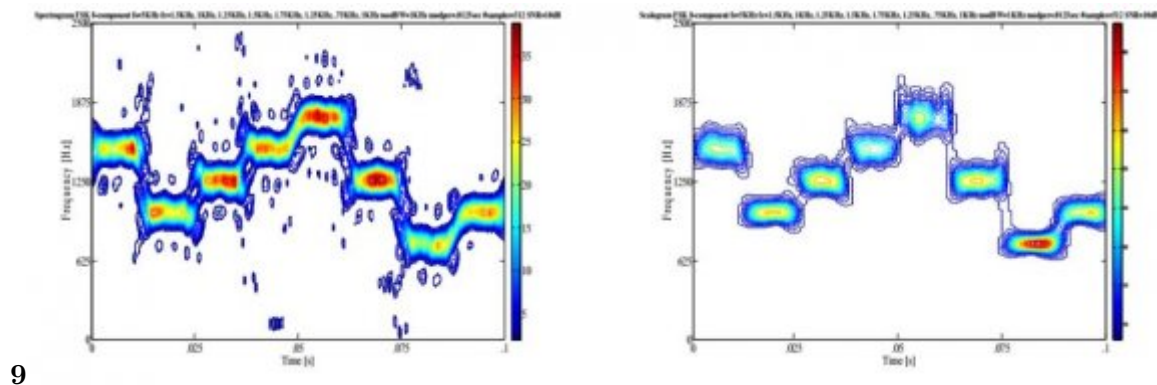
8

Figure 10: Figure 8



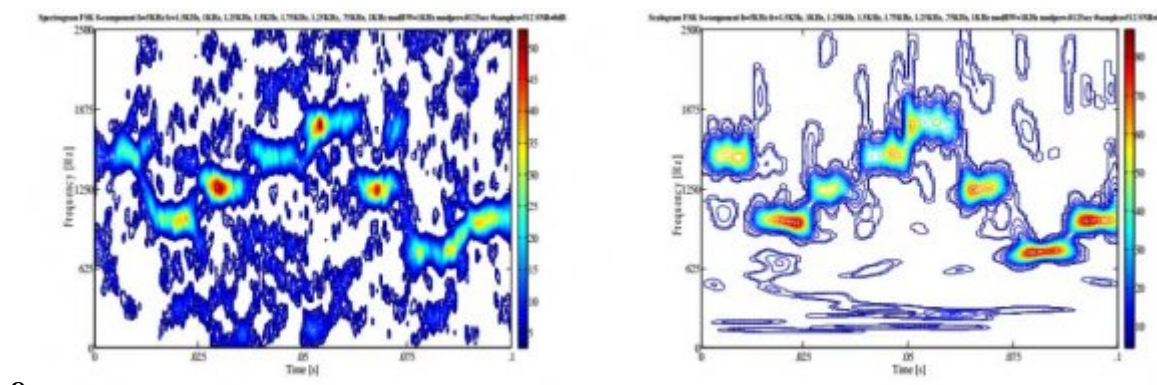
8

Figure 11: Figure 8 :



9

Figure 12: Figure 9



9

Figure 13: Figure 9 :

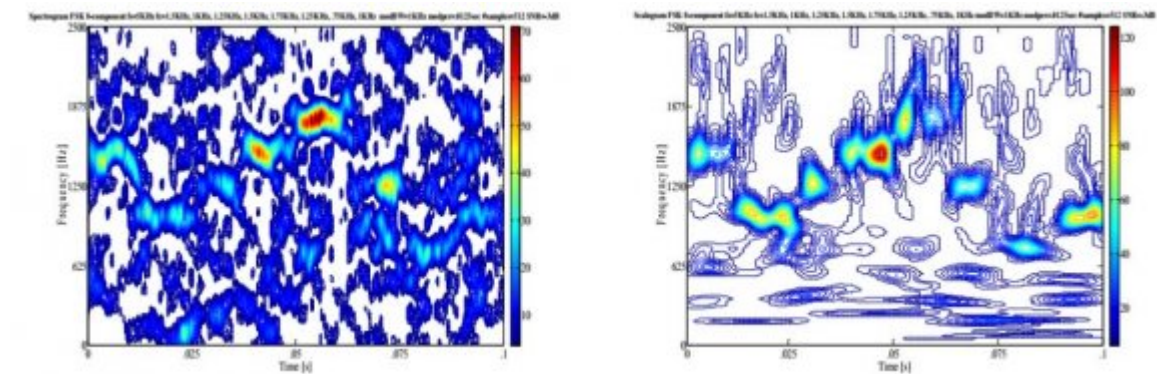


Figure 14:

1

The metrics from the Spectrogram were then compared to the metrics from the Scalogram. By and parameters carrier frequency modulation bandwidth modulation period time-frequency localization-y

Spectrogram	Scalogram
0.67%	0.44%
25.70%	21.62%
11.37%	10.25%
9.77%	9.44%

Figure 15: Table 1 :

- 220 [Farrell and Prescott ()] *A Low Probability of Intercept Signal Detection Receiver Using Quadrature Mirror Filter*  
221 *Bank Trees*, T C Farrell , G Prescott . 1996. IEEE Proceedings. p. .
- 222 [Farrell and Prescott (1999)] ‘A Method for Finding Orthogonal Wavelet Filters with Good Energy Tiling  
223 Characteristics’. T Farrell , G Prescott . *IEEE Transactions on Signal Processing* Jan. 1999. 47 (1) p. .
- 224 [Chen et al. ()] *A Novel Method for Extraction of In-Pulse Feature of Multi-Component LFM Signal*, C Chen ,  
225 M He , H Jin , H Li , Z Shen . 2009. 2009. p. .
- 226 [Anjaneyulu et al. (2009)] ‘A Novel Method for Recognition of Modulation Code of LPI Radar Signals’. L  
227 Anjaneyulu , N Murthy , N Sarma . *International Journal of Recent Trends in Engineering* May 2009. 1  
228 (3) p. .
- 229 [Xia and Chen (1999)] ‘A Quantitative SNR Analysis for the Pseudo Wigner-Ville Distribution’. X Xia , V Chen  
230 . *IEEE Transactions on Signal Processing* October, 1999. 47 (10) p. .
- 231 [Zhang and Jiao (2000)] ‘A Simple Method for Designing Pseudo QMF Banks’. Z Zhang , L Jiao . *Proceedings of*  
232 *the IEEE International Conference on Communication Technology*, (the IEEE International Conference on  
233 Communication Technology) Aug. 2000. 2 p. .
- 234 [Gal05] alleani et al. (2006)]b10 ‘A Time-Frequency Approach to the Adjustable Bandwidth Concept’. [ Gal05]  
235 Galleani , L Cohen , L Noga , A . *Digital Signal Processing* Sept. 2006. 16 (5) p. .
- 236 [Sat98] arkar and Su (1998)]b29 ‘A Tutorial on Wavelets from an Electrical Engineering Perspective, Part 2:  
237 The Continuous Case’. [ Sat98] Sarkar , T Su , C . *IEEE Antennas and Propagation Magazine* December  
238 1998. 40 (6) p. .
- 239 [Goh and Lim (2000)] ‘A WLS Algorithm for the Design of Low-Delay Quadrature Mirror Filter Banks’. [goh00]  
240 Goh , C Lim , T . *Proceedings of the IEEE International Symposium on Circuits and Systems*, (the IEEE  
241 International Symposium on Circuits and Systems) May 2000. 1 p. .
- 242 [Wei et al. (2003)] ‘Analysis of Multicomponent LFM Signals Using Time-Frequency and The Gray-Scale Inverse  
243 Hough Transform’. G Wei , S Wu , E Mao . *IEEE Workshop on Statistical Signal Processing* September 28  
244 -October 1, 2003. p. .
- 245 [Lari and Zakhor (1992)] ‘Automatic Classification of Active Sonar Data Using Time-Frequency Transforms’.  
246 F Lari , A Zakhor . *Proceedings of IEEE-SP International Symposium on Time-Frequency and Time-Scale*  
247 *Analysis*, (IEEE-SP International Symposium on Time-Frequency and Time-Scale AnalysisVictoria, BC) Oct.  
248 4-6, 1992. p. .
- 249 [Grishin and Janczak ()] ‘Computer-Aided Methods of the LPI Radar Signal Detection and Classification’. Y  
250 Grishin , D Janczak . *Proc. of SPIE*, (of SPIE) 2007. 6937 p. .
- 251 [Conference Record of the Twenty-Eighth Asilomar Conference on Signals, Systems and Computers ()]  
252 *Conference Record of the Twenty-Eighth Asilomar Conference on Signals, Systems and Computers*,  
253 1994. p. .
- 254 [Zahhad and Sabah ()] ‘Design of Selective M-Channel Perfect Reconstruction FIR Filter Banks’. A Zahhad , M  
255 Sabah . *IEE Electronics Letters* 1999. 35 (15) p. .
- 256 [Pace ()] *Detecting and Classifying Low Probability of Intercept Radar*, P Pace . 2009. Norwood, MA: Artech  
257 House.
- 258 [Papandreou et al.] *Detection and Estimation of Generalized Chirps Using Time-Frequency Representations*, A  
259 Papandreou , G F Boudreaux-Bartels , S Kay .
- 260 [Hippenstiel et al. (2000)] *Detection and Parameter Estimation of Chirped Radar Signals. Final Report, Naval*  
261 *Postgraduate School*, R Hippenstiel , M Fargues , I Moraitakis , C Williams . Jan. 10, 2000. Monterey, CA.
- 262 [Mitra ()] *Digital Signal Processing, A Computer-Based Approach, Second Edition*, S Mitra . 2001. Boston, MA:  
263 McGraw-Hill.
- 264 [Adamy ()] *EW 102: A Second Course in Electronic Warfare*, D Adamy . 2004. Norwood, MA: Artech House.
- 265 [Gulum et al. (2008)] ‘Extraction of Polyphase Radar Modulation Parameters Using a Wigner-Ville Distribution-  
266 Radon Transform’. T Gulum , P Pace , R Cristi . *IEEE International Conference on Acoustics, Speech, and*  
267 *Signal Processing*, (Las Vegas, NV) April 2008.
- 268 [Rangayyan and Krishnan ()] ‘Feature Identification in the Time-Frequency Plane by Using the Hough-Radon  
269 Transform’. R Rangayyan , S Krishnan . *Pattern Recognition* 2001. 34 p. .
- 270 [Anjaneyulu et al. (2009)] *Identification of LPI Radar Signal Modulation using Bi-coherence Analysis and*  
271 *Artificial Neural Networks Techniques*, L Anjaneyulu , N Murthy , N ; Sarma , Iit Guwahati . 2009. January  
272 16-18, 2009. p. .
- 273 [Grishin (2008)] ‘Interferences Excision Via Time-Frequency Distribution in Radio Communication Systems’.  
274 Y Grishin . *XVIII-th International Conference on Electromagnetic Disturbances*, (Vilnius, Lithuania) 2008.  
275 September 2008. p. .

- 276 [Li and Bi ( )] X Li , G Bi . *A New Reassigned Time-Frequency Representation. 16 th European Signal Processing*  
277 *Conference*, (Lausanne, Switzerland) August 25-29, 2008. p. .
- 278 [Hlawatsch and Boudreaux-Bartels (1992)] ‘Linear and Quadratic Time-Frequency Signal Representations’. F  
279 Hlawatsch , G F Boudreaux-Bartels . *IEEE Signal Processing Mag* April 1992. 9 (2) p. .
- 280 [Al-Namiy and Nigam (2000)] ‘On the Design of 2-Band FIR QMF Filter Banks Using WLS Techniques’. F Al-  
281 Namiy , M Nigam . *Proceedings of the Fourth IEEE International Conference on High Performance Computing*  
282 *in the Asia-Pacific Region*, (the Fourth IEEE International Conference on High Performance Computing in  
283 the Asia-Pacific Region) May 2000. 2 p. .
- 284 [Li and Xiao (2003)] ‘Recursive Filtering Radon-Ambiguity Transform Algorithm for Detecting Multi-LFM  
285 Signals’. Y Li , X Xiao . *Journal of Electronics (China)* May 2003. 20 (3) p. .
- 286 [Sar98] arkar and Su (1998)]b28 [ Sar98] Sarkar , T Su , C . *Discrete Wavelet Techniques. IEEE Antennas and*  
287 *Propagation Magazine*, October 1998. 1 p. .
- 288 [Han et al. (2000)] ‘Target Position Extraction Based on Instantaneous Frequency Estimation in a Fixed-Reticle  
289 Seeker’. S Han , H Hong , D Seo , J Choi . *Opt. Eng* September 2000. 39 p. .
- 290 [Cohen ( )] ‘The Wavelet Transform and Time-Frequency Analysis’. L Cohen . *Debnath, L., Wavelet Transforms*  
291 *and Signal Processing*, 2002. Birkhauser. p. .
- 292 [Boashash ( )] *Time Frequency Signal Analysis and Processing: A Comprehensive Reference*, B Boashash . 2003.  
293 Oxford, England: Elsevier.
- 294 [Cohen ( )] *Time-Frequency Analysis*, L Cohen . 1995. Upper Saddle River, NJ: Prentice Hall.
- 295 [Ozdemir (2003)] *Time-Frequency Component Analyzer. Dissertation*, A Ozdemir . Sept. 2003. Ankara, Turkey.  
296 Bilkent University
- 297 [Auger et al. ( )] *Time-Frequency Toolbox Users Manual*, F Auger , P Flandrin , P Goncalves , O Lemoine . 1996.  
298 Centre National de la Recherche Scientifique and Rice University